DOI 10.2478/ama-2025-0003 acta mechanica et automatica, vol.19 no.1 (2025)

STATIC CARRYING CAPACITY OF A SINGLE-ROW BALL SLEWING BEARING TAKING INTO ACCOUNT DRIVE TRANSMISSION CONDITIONS

Szczepan ŚPIEWAK*

*Faculty Of Mechanical Engineering And Computer Science, Institute Of Mechanics And Machine Design, Czestochowa University of Technology,Dabrowskiego Street 73, 42-201 Czestochowa, Poland

e-mail: szczepan.spiewak@pcz.pl

received 18 January 2024, revised 10 March 2024, accepted 01 April 2024

Abstract: Problems of computing a slewing bearings static carrying capacity have been presented in the paper. Particularly it was concentrated on determination of static limited load curves which include axial forces, radial forces and tilting moments. A calculation were performed on the base of single-row ball slewing bearing with four-point contact zone. In this work a procedure of determining the static limiting load curves on the basis of modeling by using the finite element method (FEM), analytic Eschmann's formulas and classical mechanics equations have been described. The structure of FEM bearings' model was considered with gear conditions between a toothed bearing's ring (rim) and a drive pinion in a power train of the excavator F250H symbol. Moreover, in the model flexibility of: the bearing rings, a contact zone ball-bearing, support structure and mutual interactions between bolts clamping the bearing rings and the support structures were taken into account. The static carrying capacity of the analyzed bearing, considered with the pinion and without was compared. Quantitative assessment of loads of the contact zones ball-raceway was achieved by using a statistic criterion.

Key words: slewing bearing, bearing capacity, bearing design, tilting moment, static limiting load curves, the toothed ring

1. INTRODUCTION

Machine rolling bearings selection is normally based on an assumed durability. Estimated external loads are initially converted to two main loads. The first load is a vector projected on rotation axis of the bearing (an axial force) and the second load is the vector (radial force) directed perpendicular to the first load. The main loads are then combined to the value of equivalent load which depends on the type of bearing rolling elements and desired durability, what allows to estimate required dynamic carrying capacity. The operating bearing conditions determine whether selection of the bearing is dependent on the value of a static or a dynamic carrying capacity. In order to minimize the bearing dimensions, the designed solutions of the bearing raceways have been shaped in such a way, in order that the given bearing adapt to one of the main loads. In practice, it can be interpreted that greater value of the main loads will determine a choice of the bearing type (in practice, it can be interpreted that greater value of the main loads, will determine a choice of the bearing type (between a radial and an axial bearing). Among the rolling bearings, slewing bearings play a more responsible role, especially when it is used in large-scale machines. In these types of rolling bearings, the external loads are combined similarly like in bearings, designed for general use. While bearing is being selected, all resultant forces may be projected into axial (axial force Q) and radial (radial force H) directions while a tilting moment M [1, 2] is a specific load of this rolling bearing type. In typical applications of slewing bearings, permissible external bearing load is dependent on static carrying capacity. The static carrying capacity of rolling bearings is determined by the deformation of the contact zone between the rolling element and raceway hence and then the so-called static carrying capacity characteristic is determined for newly designed slewing bearings. The characteristic is graphically presented as dependence of the tilting moment M from the axial force Q while the system is loaded by a constant value of the radial force H [2-7]. Such way of presenting the slewing bearing serviceability results from the following designed features (specifically distinguishing the slewing bearings from bearings in general use): assembly in support structures by means of bolts, track diameters which can be in a range of several meters, bearing rings load of high axial forces, high radial forces and high tilting moment, high deformability of a contact zone rolling element-raceway, application of various materials for the production of bearing rings and rolling elements, low-speed rotation of the rings, a large number of balls and / or rollers, in some systems - toothed rim incised on circumference of the one ring. Engineers use these curves when slewing bearing is selected for load conditions of machines [3-5]. As it results from the catalog review [3, 4], static carrying capacity curves of the slewing bearings have been determined only for the zero values of radial forces H. Based on work [3], it can be stated that if the value of a radial force does not exceed 10% of the maximum permissible axial force, the course of the static carrying capacity curve will not be shifted. Another approach to the problem of taking into account the radial force was presented in Ref. [5]. The bearing manufacturer introduces the relationships used to determine the so-called equivalent tilting moment Meq and equivalent axial force Qeq. These parameters are determined on basis values of external loads M, Q, H and application coefficient, the radial force H and a safety factor. The determined values of Meq and Qeq are plotted in the catalogs of static carrying capacity curves that have been determined for zero values of a radial force. If these values are located below the curve for checked bearing then this bearing can be selected as suitable for the rated load. A detailed reference, based on the calculation example, was presented in the paper [7]. Therefore, the identification of operating conditions of slewing bearings determination requires of the radial force share in a system of external loads. An influence of the radial forces (taking into account their sense) on the static carrying capacity of the twin slewing bearing has been demonstrated in the work [2]. The same type of slewing bearing was the subject of research of the authors of the publication [8]. The researchers using a classical model based on the static equilibrium of displacements of a rigid body and assumed durability determined the dynamic carrying capacity curves of the slewing bearing, taking into account an one radial force sense [8]. The researchers using a classical model based on the static equilibrium of displacements of a rigid body and assumed durability determined the dynamic carrying capacity curves of the slewing bearing, taking into account an one radial force sense [8].

The action of the radial force on a slewing bearing may be temporary (e.g. in an excavator with one bucket [9]) or continuous as in the case of a wind turbine [10] and a wagon tippler.

The impact of operate direction of the radial forces on the static carrying capacity of the slewing bearings was presented in Ref. [11].

It should be emphasized that the slewing bearing is the transmission element of a rotational torque between the pinion and the slewing bearing ring. There is a high probability of simultaneous operation of the external load components in one plane, which is common with the plane of the pinion symmetry at a point of teeth contact.

Continuous research and development of research methods used in slewing bearing problems analysis have great practical importance because of the fact that assembly processes of the slewing bearing are time-consuming and energy-consuming (due to size and weight). Slewing bearings in drive systems play a key role. A failure of a slewing bearing causes the machine to stop for an unpredictable period of time. Therefore, machine designers have a difficult task related to the selection of a slewing bearing in terms of its type and carrying capacity. Methods of determining static carrying capacity curves of slewing bearings are similar to each other and are widely described in publications [1, 2, 6, 10, 12 13]. Each of the method boils down to determine the maximum force (reaction) which acts between the rolling element and the bearing raceway while components of the external loads (M, Q, and H) act on the bearing. Individual methods of determining the static carrying capacity of slewing ring bearings usually differ in the adopted range of bearings features which are included in created calculating models.

The basic features taken into account in the models of slewing bearings are: bearing clearance, initial clamp of bolts, flexibility of bearing rings, flexibility of a contact zone (raceway - rolling element), raceway hardness condition and bearing mounting structures susceptibility. The permissible load of a contact zone between the rolling element and raceway is a parameter that determines the carrying capacity of slewing bearings. Effect of technological treatments performed on the bearing raceways in reference to permissible carrying capacity of the contact area and durability tests are presented in the works [14, 15]. Evolution of a measurement technique based on the analysis of acoustic signals enables diagnostics and monitoring slewing bearings operation, what has been presented in the works [16, 19]. The descriptions of friction torque in slewing bearings are included in publications [20, 21]. Slewing bearings can also operate at elevated temperatures (e.g. in the Ljungstrom rotary air heater). Results of research on thermal loads of the slewing bearing can be found in the publication [22]. On the basis of the distribution of loads acting in the contact zones between rolling element and raceway, which are presented in the works [1, 6, 9, 12, 23, 24], it can be concluded that these loads cause change of bearing rings' shape and deform the slewing bearing toothed ring. Simultaneously the geometrical mating conditions between the gears change.

The gear interaction, taking into account bearing ring flexibility, will undoubtedly affect a distribution of the forces loading the bearing balls. Since the force loads of the single contact zone rolling part - raceway decide about the slewing bearing static carrying capacity, however the static carrying capacity during mating the flexible toothed ring and the rigid pinion may by another. In the literature, there is a publication which concerns bearing clearance [12], preloads [25] and the stiffness of the support structures [9] in reference to courses of the static carrying capacity curves, whereas the influence of the gear condition of the toothed ring with the pinion on the course of the static carrying capacity curves, especially with the specific direction of external loads (M and H) seems to be unnoticed. Numerical studies of action gear pinion with the toothed ring of slewing bearing were carried out and based on the presented findings. The distributions of forces acting in the individual contact zones (ball - raceway) and static carrying capacity curves of the slewing bearing were determined with and without considering the conditions of the mating between the rim and the pinion.

2. A MODEL OF A POWER TRAIN WITH THE SLEWING BEARING

Acceding to formulated problem of slewing bearing load, the single-row ball slewing bearing with the four-point contact zone (made in Poland) has been considered. The choice of this bearing for study was dictated by the fact that this bearing is mounted in one-shovel tracked excavator F250H. A comprehensive model of the working structures of a body and a chassis of the F250H excavator connected with modeling the bearing was presented in work [26]. An outline of the bearing cross-section is shown in Fig. 1 and basic design parameters are listed in Tab. 1. A power train of excavator bodywork consists of a spur gear which basic parts are the pinion assembled in the bodywork and a rim made on an external slewing bearing ring. The basic parameters of the gear have been marked in Fig.2 and listed in Tab. 2. Due to required distance between centers of gears and number of tooth of the pinion, the pair of gears have been subjected to profile shift.

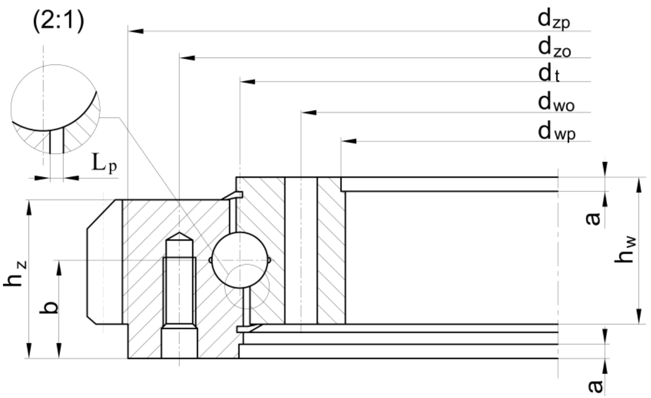

Fig. 1. Basic geometric parameters of the single-row ball slewing bearing

A sector of the profile shift was generated by using the Inventor program. Take into account complexity of the task posed, it was decided that the numerical calculations is based on the finite element method (FEM). In comparison with the analytical methods (classical) in which the main goal is idealization of the flexural-torsional stiffness of the bearing rings [6, 25] - FEM allows to take into account not only compliance of the bearing rings, but also compliance of the bearing bolts and compliance support structures.

Tab. 1. Values of basic parameters of the single-row ball slewing bearing

	Parametr of the bearing	Value
1	The track diameter of the bearing d_t [mm] (Fig. 1)	1105
2	The ball diameter d_k [mm]	44
3	Quotient rays of ball and receway k_p [2, 34]	0,96
4	Dimension d_{zp}[mm] (Fig. 1)	1260
5	Dimension d_{zo} [mm] (Fig. 1)	1200
6	Dimension d_{wo}[mm] (Fig. 1)	1010
7	Dimension d_{wp} [mm] (Fig. 1)	960
8	High of the bering h [mm]	137
9	Dimension a [mm] (Fig 1)	10
10	Dimension b [mm] (Fig. 1)	71
11	Dimension h_w [mm] (Fig. 1)	117
12	Dimension h_z [mm] (Fig. 1)	122
13	Axial clearance [mm]	0,5
14	The clearance between the rings L_p [mm] (Fig. 1)	7
15	Nominal contact angle α_o[°]	45
16	Row fill facctor	0,83
17	Number of bearing balls	64
18	The surface balls hardness	62HRC
19	The surface raceway hardness	56HRC
20	Number of the bolts mounting in the internal/external ring	42/42
21	The size and strength class mounting bolts by [DIN] [31]	M24-12.9
22	Mounting tension force S_w [kN]	242

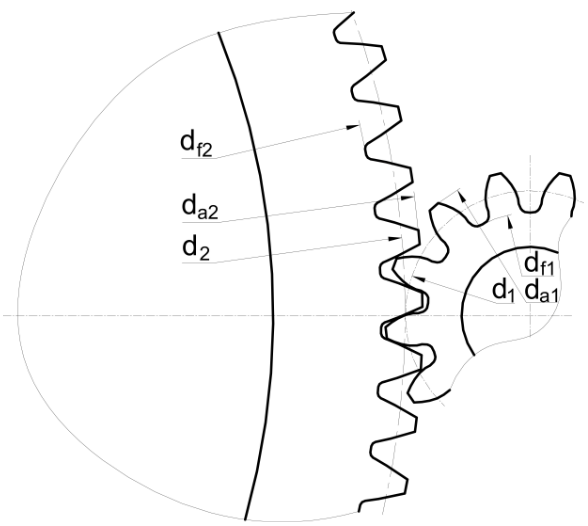

Fig. 2. The basic geometric parameter of a pinion and a toothed ring

In addition, in the case of the classical methods [6, 25], the relative displacement of the bearing rings caused by the loads have been considered as motion of a rigid body. In a slightly different way the susceptibility of the roller section- raceway contact zone have been defined.

According to above paragraph, with data contained in Tab. 1, a comprehensive model MES of single-row ball slewing bearing with the pinion in the environment of the ADINA [27, 28] have been developed, and presented as a mesh in a Fig 3.

Tab. 2. Values of gears basic parameters

	Name of parameters	Pinion	Toothed rim
1	Reference diameter [mm]	d_1=182	d_1=1274
2	Tip diameter [mm]	d_{a1}=211,763	d_{a1}=1322,823
3	Root diameter [mm]	d_{f1}=151,577	d_{f1}=1262,637
4	Profile shift coefficient	x_1=0,1135	x_2=0,7942
5	Number of tooth	z_1=13	z_2=91
6	Module [mm]	m=14	
7	Backlash [mm]	j_n=0,56	
8	Center distance [mm]	a_w=740	
9	Reference pressure angle	α_n=20°	
10	Working pressure angle	α_w=22,414°	

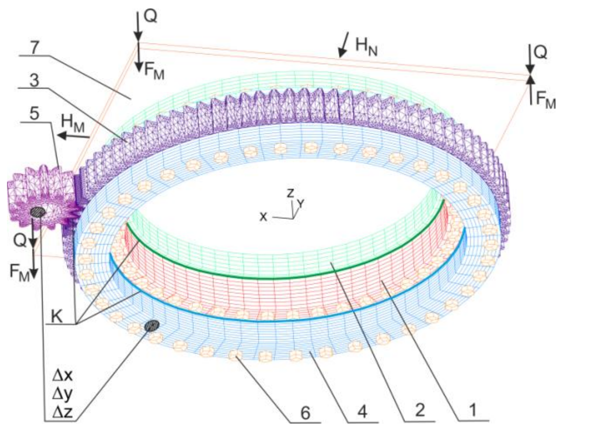

Fig. 3. A visualisation of finite elements of single-row ball slewing bearing, coupled with a drive pinion

The Fig. 3 shows: 1 - the bearing inner ring, 3 - outer ring, 2 - the upper and 4 - lower support structure, 6 - heads of the mounting bolts, and 7 - plate which have been discretized by eight-nodal finite elements type 3D-Solid [27-28], whereas 5 - the pinion and 3 - the toothed rim were discretized by twelve-nodal finite elements.

The mating conditions' model between the toothed ring and the pinion was based on the methods of tooth profile discretization presented in [29] and the issues of the teeth contact strength [30].

In order to modeling balls by using replacement elements (described below), the bearing rings were discretized by finite elements arranged in the shape of slices. Number of these slices is equal to the number of balls in the bearing. The angular scale of the slice overlaps with the angular scale of a position of the balls in the bearing. Between the upper support structure and the inner ring and between the lower support structure and the external ring conditions of contact K (including the penetration condition and friction coefficient value μ= 0,1 [27, 28]) were defined as well as between a contour gear of the pinion and the bearing rim. Nodes containing the flat surface of the lower cover have been taken all degrees of freedom (Δx, Δy, Δz = 0). Similarly it was done in case of nodes describing a cylindrical pinion surface on which a drive shaft is mounted.

External load has been identified through FM, Q, HM, HN vectors. The static carrying capacity curve is determined as standard for the main system of forces M, Q, HM [11]. In the case under consideration, symmetry slewing bearing YZ plane was used to modeling the tilting moment and two opposite vectors of forces FM. The vector Q represents the axial force. Since the system of forces in the model enables consideration of radial forces, the following nomenclature is adopted: a major radial force HM and orthogonal radial force HN.

In the present task the main system of forces is contained in the pinion plane of symmetry at a point of tooth contact. The vectors of simulated loads have been hooked in the nodes one - element group of finite elements with No. 7. Group of finite elements with No. 7 was specially created as an object (plate plane) that intermediate during transmitting the load to support bearing structure (No. 2 and No.4). Nodes of group No. 2 contained in the plate plane 7 gave the conditions of displacements glue type [27]. This type boundary conditions are defined for elements of group No. 6, mapped the heads of the mounting screws and for rim coupled with outer ring. Boundary glue type conditions ensure an agreement of all displacements for all nodes which coordinates are contained in the same flat surface. The bolts have been modeled by finite elements type beam with an active bolt function [27]. The nodes of the individual beam type finite elements have been connected with finite elements of group No. 6 which represents the ends of the bolts and nuts in an assembly of the bearing and housing. Only in this way, the necessity to map the holes in the bearing rings was avoided, e.g. by defining discontinuities in the structures between the finite elements of groups no. 1, 2, 3, 4. This simplification reduces the number of finite elements and an accuracy of a calculation results in the static carrying capacity range are sufficient. An additional advantage is the shorter calculation time. Activation of the bolt function in the ADINA system enables definition of the bolt diameter, material parameters and mounting tension force [27] Sw (Tab. 1). Based on these data, the ADINA solver [27] during initial iterations calculates displacement caused by the Sw forces (according to guidelines of standard [31]) for all model nodes. In this case the slewing bearing is seated in an annular housing with the centering collar. Such a solution requires more precise shaping of the support structure, but in the system it reduces the transverse loads of bolts (reduction of shear stress). The dimensions of the support structure must ensure the appropriate system stiffness and are parametrically dependent on the bearing dimensions [3]. Those dependents was taken into account in the model during setting the dimensions of element no. 2 and 4. However, the most important simplification in the bearing model is balls replaced by an alternative finite element system called superelements [32, 33]. As it is shown in Fig.4 the superelements consisted of beam system 2 with a high stiffness combined with truss elements 1, where the end nodes are located in the curvature centers of the bearing raceways 3 (points: A, B, C, D) and the nodes of finite element meshes of the internal and external rings. The truss elements 1 have defined multilinear material characteristics. A method of determining the necessary material characteristic is described in detail in [2]. Other statistical data regarding sizes of finite elements, the number of finite elements, and the sensitivity analysis of finite elements have been included in Appendix B.

Material characteristics shall be determined on the basis of contact zone characteristics. Characteristics of the contact zone is defined as dependence the raceway deflection η caused by a contact rolling section force F.

This dependence can be:
– defined by carrying out on the basis of experiment,
– based on average over the values of the c and w coefficients and inserted into the formula 1, which sample values are function of osculation ratio kp to the roller bearing raceway what can be bring out from work [1]
– defined as a solution to the question of contact issue of the contact zone by using the finite element methods.

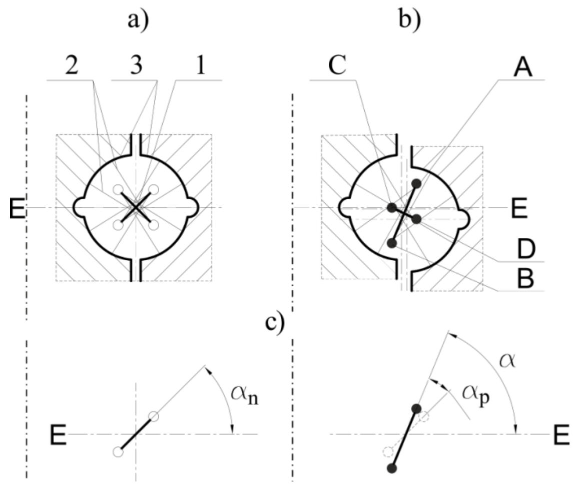

Fig. 4. Schematic position of bearing rings and replacement elements in a state before (a) and after (b) load inflicted with mapping changing of contact angle of balls in slewing bearing (c)

$$\eta = cF^w \tag{1}$$

It should be emphasized that the characteristics of rolling bearing contact zone is also shown as the dependence of the maximum normal stress at the interface between the rolling pairs in the function of the proper load of the roller part (which is the quotient of force and the square of roller part diameter) which is wider described in [9].

Use of one of the two equivalent quality descriptions of the characteristics of the contact zone can be identified with respectively two equivalent criteria for determining the load capacity of a single contact zone:
– the criterion of plastic deformation in the contact zone,
– the criterion of maximum pressure values on the surface of the contact zone.

This study was based on the criterion of the permissible plastic deformation in the contact zone which, in accordance with the assumptions [34] should not exceed 0,0002dk. Hence, the maximum force value, which is allowed for a single ball-raceway contact zone was calculated in accordance with equation 2 [34] and amount F_{dop} = 158 kN.

$$F_{dop} = \frac{9{,}9626 \cdot 10^7 \cdot d_k^2 \cdot \left(\frac{HV}{750}\right)^2}{\left(\frac{858}{a_H b_H} \sqrt[3]{d_k \left(\frac{4-2k_p}{d_k} + \frac{2\cos\alpha_0}{d_t - d_k \cos\alpha_0}\right)}\right)^2} \tag{2}$$

The names of the formula symbols are given in the table 1. The remaining symbols represent the formula: a_H, b_H- coefficients of the elliptical contact area by [21], HV- raceway surface hardness of Vickers scale.

In contrast, the characteristic of the replacement contact zone of the bearing implemented in the model was determined according to the method described in [2] and is presented in Fig. 5. Additional information regarding, among others, the finite element mesh parameters of the contact zone model have been included in Appendix B.

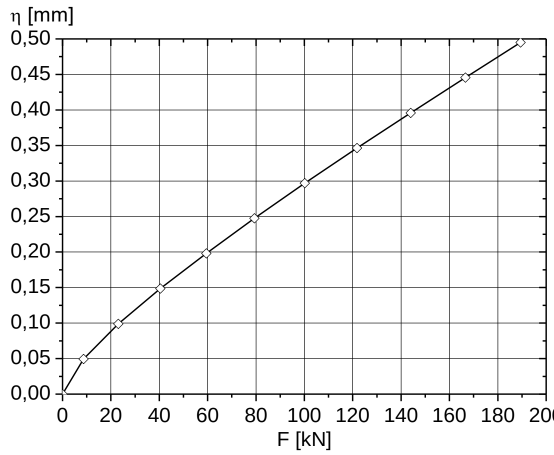

Fig. 5. Characteristic of the contact zone replacement

The system of bearing model placeholders was represented by local deformations occurring in the ball-raceway contact zone and the change of contact ball angle and consequently allows for the appointment of distributions of the reactions acting on all balls in bearing rows. Knowledge of distribution of the forces acting on each of contact zone allows to build a static carrying capacity curve, because its carrying capacity is determined by the most loaded ball, and downforce balls into the raceway is not greater than the F_{dop}.

3. STATIC CARRYING CAPACITY CURVES OF THE SLEWING BEARING

Taking into consideration the issues which have been previously identified, the impact of the radial forces and the sense of the main radial force on the slewing bearing static carrying capacity has been taken into account. Identification of force sense was associated with the sign of its value what is contractual in nature and was suggested in [11]. This work shows that sense of the main radial force have significant impact on the course of the static carrying capacity curve of the single-row ball slewing bearing. In order to make the sign of the main radial force H_M independent on an adopted local coordinate system and other directions and senses of an external loads, a definition of the main radial forces H_M directed positively was formulated. In this situation, the attention is focused on the most heavily loaded contact zone. During calculations, when increase of the main radial force cooperating with the tilting moment and the axial force causes increase load in the considered contact zone, then the main radial force is called as directed positively. Whereas, when the load of this contact zone is decreases then the sense of the main radial force is considered as negative (main radial force directed negative positively). If an orthogonal radial force H_N replaces the H_M force in the main load system, then the orthogonal radial force does not identify sense because the sense of this force has no effect on the course of the static carrying capacity curve. Points of the static carrying capacity curves are determined an iterative manner. At the beginning of calculation in the FEM model, the individual components of the external load *M*, *Q*, *H* were asked incrementally (according with the individual values of time steps *t)*. As an effect of iterations, incremental growth of the external loads generated the distribution of resultant reaction of the individual contact zones. Series of calculations were ended when one reaction acting at the point of contact ball with the raceway was equal to the force limit F_{dop}.

A full static limiting load curves of the slewing bearing have been presented in Figures A1-A4 [11] (Appendix A) but without taking into consideration the gear conditions. These charts show the influence of radial forces (specifically directed) on courses of bearing static carrying capacity curves (*Q*, *M*). A significant loss of static carrying capacity is caused by the radial forces H_N directed orthogonally and the radial forces H_M directed positively (Fig. A1). On the basis of these results (*Q*, *M*), for given radial forces H_N (Fig. A4) and H_M (positively – Fig. A2 and negatively - Fig. A3 directed), using the model presented here, comparative calculation were performed. It was concluded that plane created during the main system of forces is the plane of pinion symmetry the radial forces H_M (directed negatively) and H_N does not cause a change of the bearing static carrying capacity. A loss of the static carrying capacity occurs when the radial force H_M is directed positively. This is especially noticeable when the radial force H_M is about 15% of the maximum allowable axial force Q_{max} (M=0, H_M=0, H_N=0). In considered case the bearing radial force is H_M=1,120 [MN]. This load was implemented in the FEM slewing bearing model (Fig. 3) with taken into account gear condition. The static carrying capacity curve was determined for this load. In Fig. 6 there are shown courses of the static carrying capacity load curves of the slewing bearing with and without taken into consideration gear condition.

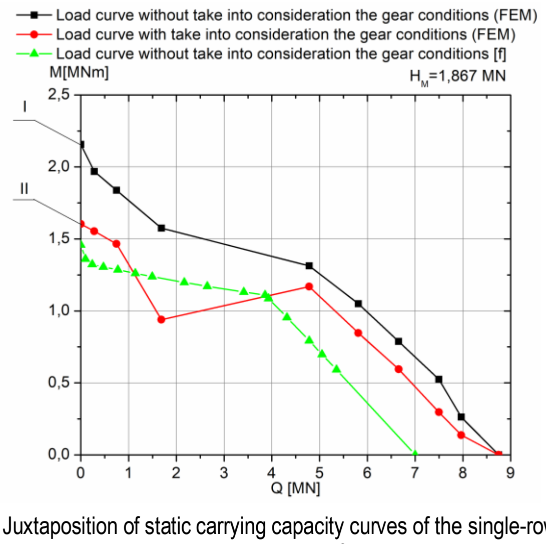

Fig. 6. Juxtaposition of static carrying capacity curves of the single-row ball slewing bearings loaded by radial forces directed positively with and without taken into consideration gear condition

In order to identify the potential causes of the presented problem, the distributions of forces acting on the individual ball - raceway contact zone of analyzed bearing for selected characteristic operation points (I and II marked in Fig. 6) have been shown in Fig. 7. The maximum allowable radial force for the assumed simulation conditions has been amounted at the level of H_{max}=3,3 [MN]. Whereas in case when the gear condition was omitted, a maximum value of the allowable radial force has been amounted H_{max}=5,977 [MN]. Decrease of H_{max} value is an effect of a distribution of the forces loading of balls. The distribution of forces acting

DOI 10.2478/ama-2025-0003

on the individual contact zone ball - raceway for both cases modelled bearings have been presented in Fig. 8.The elements of statistics were used for a quantitative assessment, allowing to describe the nature of load of the bearing contact zones and at the same time to determine the origin of the course of the considered static carrying capacity curve. In the presented bearing a four-point raceway-ball-raceway contact zone is identified.

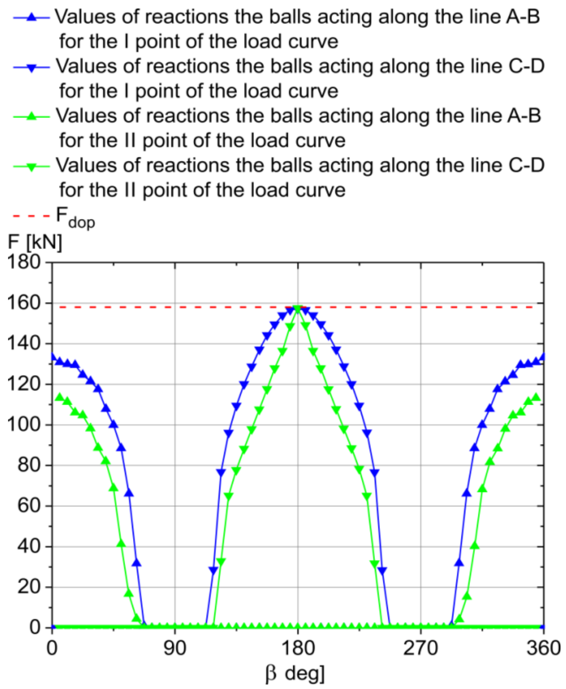

Fig. 7. Comparison of distributions of the forces acting on balls of the single-row ball slewing bearing for the points of work: I and II according to Fig. 6, β- angular coordinate

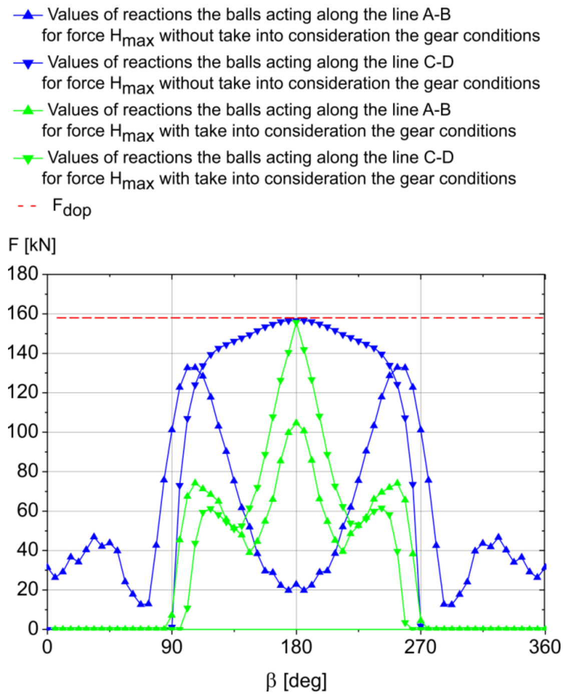

Fig. 8. Comparison of distribution of the forces acting on balls of the single-row ball slewing bearing for the maximum radial force with taken into consideration (H_{max}=5,977 [MN]) and without(H_{max}=3,3 MN) the gear condition, β- angular coordinate

During the complex state of external loads of the slewing bearing, some of contact pairs do not carry the load so zero values of forces acting on balls during the machining of the statistical distribution of balls reactions have been omitted. An arithmetic average (Eq. 3) and the standard deviation (Eq. 4) was determined on the basis of identified values (variance).

$$\bar{F} = \frac{\sum_i^n F_i}{n} \Leftrightarrow F_i > 0 \tag{3}$$

$$\Delta F = \sqrt{\frac{\sum_i^n \left(F_i - \bar{F}\right)^2}{n-1}} \tag{4}$$

where: F_i [N] – forces acting on balls (balls reactions of the single-row ball slewing bearing), n – number of compressive forces of the balls (values greater than zero)

These values (for the presented in Fig. 7 and 8 of the distribution of balls reactions) have been listed in Tab. 3.

Similar FE models of slewing bearings installed in heavy-duty machines were experimentally verified by the authors of the works [35, 36, 37]. Since methodology for modelling slewing bearings presented in this article is based on the same assumptions, additional experimental verification of the model was not conducted.

It should be emphasized that formula 2 was determined based on experimental tests of the load capacity of a contact zone for the system ball-raceway.

In order to check the obtained results (similarly as in work [13]), the static carrying capacity curve of the slewing bearing was determined using a classical method called by the authors of the work [38] - the continuous loading method. Since this method does not make it possible to take into account the conditions of cooperation between a toothed bearing's ring and a drive pinion, the additional curve presented in Fig. 6 can be compared with the curve obtained based on the FEM model and described as: load curve without taking into consideration the gear conditions. This curve according to the model [38] gave an intermediate solution in the presented case.

4. SUMMARY

On the basis on performed simulation, made by developed bearing model including gear conditions, it is found that the operation of the radial forces directed to the pinion causes a decrease of the static carrying capacity of the slewing bearing. Therefore an area of work described as a course of static carrying capacity curve of the slewing bearing cooperating with a pinion and loaded by positive radial force is smaller. H_{max} force is smaller about 45%, and M_{max} value (Fig. 6) for the H_M value amounts only 15% Q_{max}, is smaller about 27%.

A review of the load distribution for individual load conditions in both models allows to explain the loss of the bearing static carrying capacity.

According to statistical evaluation criterion of the strength properties of the slewing bearings (more widely presented in the work [11]) for the gear condition of the rim and the pinion, the values of arithmetic averages of ball reactions at contact points with the raceways are much smaller than in case of model without pinion. Thus, higher loads are accumulated to the smaller number of pairs of contact. According to the statistical criterion of slewing bearings, the best load conditions for the contact zones between balls and raceways occur when the mean values of the ball reaction are as high as possible, and the values of the standard deviation as low as possible.

Tab. 3. Juxtaposition of statistical parameters describing the nature of the load of ball of single-row ball slewing bearing (Fig. 8) for the selected points of work I and II (Fig. 7)

Model of bearing	External load components			Number of forces	Ball reaction values F_i	
	Q [MN]	M [MNm]	H_M [MN]		Arythmetic average [kN]	Standard deviation [kN]
Without pinion	0	1,603	1,120	49	108,7	40,7
With pinion	0	2,156	1,120	44	89,5	38,6
Without pinion	0	0	H_{max}=3,3	98	81,4	52,4
With pinion	0	0	H_{max}=5,977	63	65,5	31,5

Limitation of the static carrying capacity also arises from the condition of contact strength of the pinion and rim and it will be the subject of an another publication in this scope. During a deformation of a bearing ring the contour of the deformed toothed ring differs from a circular outline and causes that a distribution of the contact pressures along the side surface of the tooth is irregular. The distribution of displacements in the direction of the radial force H_M for operation points marked in Fig. 6 as II is shown in Fig. 9. The orthogonal projection (on the XY plane) of the deformed profile of the toothed ring has a shape which can be approximated as an ellipse. The reasons for such state are both - the condition of the external load (Q, H_M, M) and a limitation of displacements caused by the mating conditions between the toothed ring and the pinion (forces resulting from a contact of the teeth). The most loaded contact zone of the ball-raceway (Fig. 7) is located on the direction of the line connecting the rotational axes of the toothed ring and pinion.

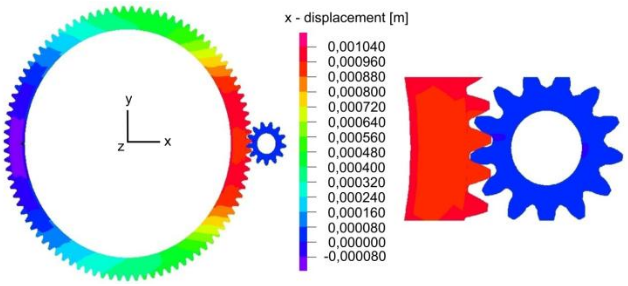

Fig. 9. The distribution of displacements in the direction of the radial force H_M for operation points marked in Fig. 6 as II

As a result of the identified deformations the working pressure angle α_w is decreased. These phenomena also has an impact on teeth strength.

The conditions of load external considered for the slewing bearing assembled in the structures of the one-shovel tracked excavator are extremely dangerous. Such a state of loads (not stipulated in the standards [3-5]) in the machine may be uncommon, but in specific operating conditions it may appear cyclically. Therefore, when the slewing bearing is selected, this issue should be taken into account. If the bearing cannot be adjusted to such extremely loads, a system should be protected against the possibility of indicated dangerous loads' cumulation.

The use of FEM for modeling a phenomena occurring in slewing bearings has many advantages over classical methods.. The most important advantage is the ability to easily increase the number of implemented parameters which changes can be analyzed, e.g. the axial clearance, the mounting tension force, selection of the number of bolts, dimensions of support structure.

The presented model of the slewing bearing complements the missing features of the model presented by author of this work in the previous article [2]. Compared to the models of other authors (Tab. 4), the slewing bearing model was expanded to include defined conditions of cooperation between a toothed bearing's ring and a drive pinion , taking into account the contact conditions between the teeth. The characteristics of the contact zone (Fig. 5) were determined using a material model of the ball and raceway, taking into account the elastic-plastic state.

Tab. 4. Overview of features characterizing individual FE models of slewing bearings against the model presented in the article [*]

Feature of the presented model		Reference number
1	The use of replacement elements for modeling rolling parts	[1], [2], [7], [9], [11], [13], [15], [18], [24], [25], [26], [32], [33], [35], [36], [37], [38],[*]
2	Taking into account the support structures in slewing bearings	[2], [7], [9], [10], [11], [25], [26], [32], [33], [35], [36], [38], [*]
3	Taking into account interactions between the bearing and bolts	[1], [2], [7], [9], [11], [13], [25], [26], [32], [33], [35], [36], [38], [*]
4	Taking into account flexible rings	[1], [2], [7], [9], [10], [11], [13], [15], [18], [24], [25], [26], [32], [33], [35], [36], [37], [38], [*]
5	Taking into account of radial forces	[1], [2], [7], [9], [10], [11], [13], [15], [18], [24], [25], [26], [32], [33], [35], [36], [38], [*]
6	Modeling of the contact zone taking into account the elastic-plastic material model	[2], [7], [11], [15], [18], [24], [26], [33], [35], [36], [*]
7	Modeling of the bearing taking into account the cooperation conditions between a toothed bearing's ring and a drive pinion	[*]

DOI 10.2478/ama-2025-0003

Appendix A

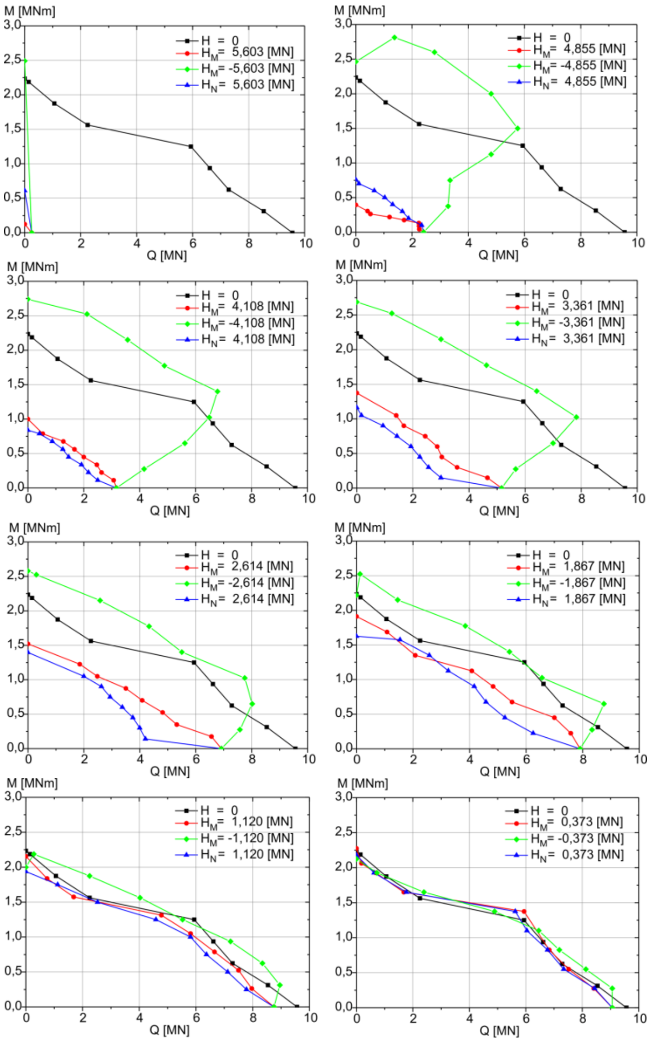

Fig. A1. Juxtaposition of static carrying capacity curves of the single- row ball slewing bearing loaded by constant values of the radial forces defined positively, negatively and orthogonaly

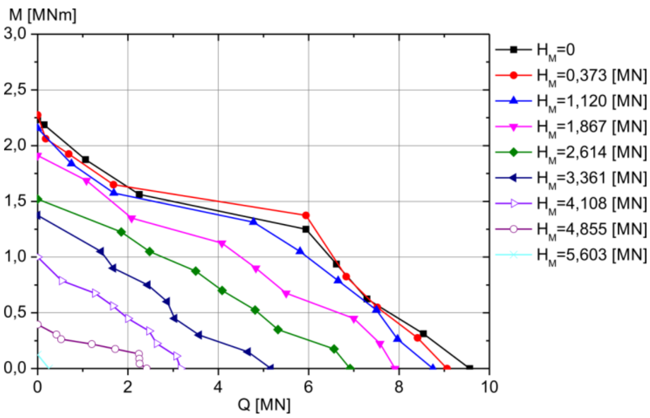

Fig. A2. Juxtaposition of static carrying capacity curves of the single-row ball slewing bearing loaded by the main radial forces H_M defined positively

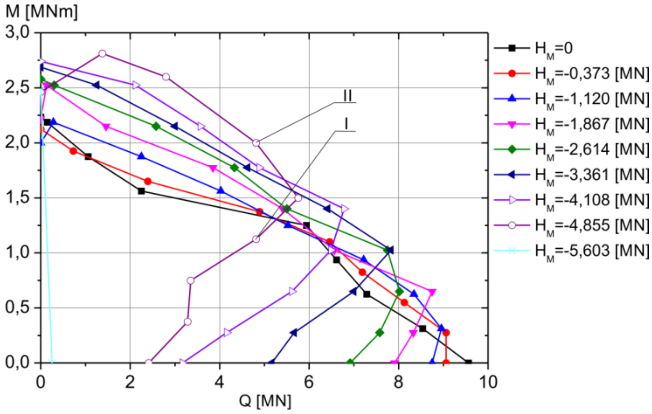

Fig. A3. Juxtaposition of static carrying capacity curves of the single-row ball slewing bearing loaded by the main radial forces H_M defined negatively

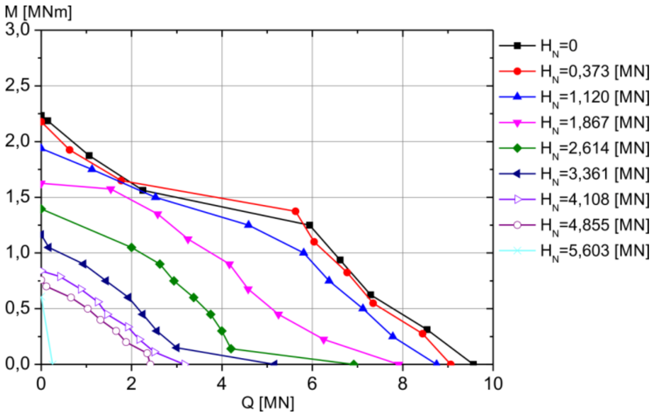

Fig. A4. Juxtaposition of static carrying capacity curves of the single-row ball slewing bearing loaded by radial forces *HN* defined orthogonally

Appendix B

A specific feature of the FEM modeling method used for the presented slewing bearing is an application of two models. The first model, called the contact zone model, is used to determine replacement characteristics of the contact zone (Fig. 5). Assumptions regarding the selection of geometric and material parameters, boundary conditions and loads have been described in detail in [2]. Output date obtained from this model is then implemented (as multilinear material characteristic of the finite element type truss) to the second model, which is the slewing bearing model. This division of tasks cause that a problem of deformation of the ball and the raceway enough to solve only once, and the solution result is used to modeling all contact pairs (ball - raceway) as the replacement elements (Fig. 4). The advantage of this method is the reduction in the number of finite elements representing a curvature of the bearing raceway, which causes a reduction of calculation time of the carrying capacity. The consequence of the method used is the need to check the influence of discretization density of geometric objects of the slewing bearing on calculation results. Taking into account the example contained in [37] and a structure of the presented bearing FE model, where several types of finite elements were used, analysis of the mesh sensitivity was focused on the following structures: a contact zones ball-raceway, a bearing ring and a gearing system. In each case, three different mesh densities were tested and described in Figures B1, B2, B3 as minimum, average and maximum density of FE mesh

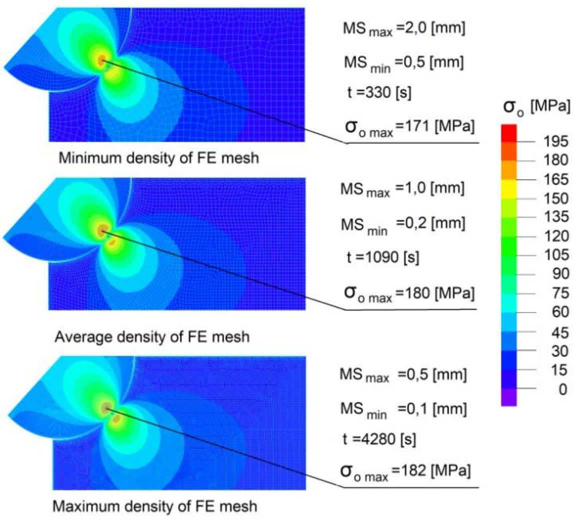

Fig. B1. Distributions of the effective stress for the tested meshes of the contact zone model

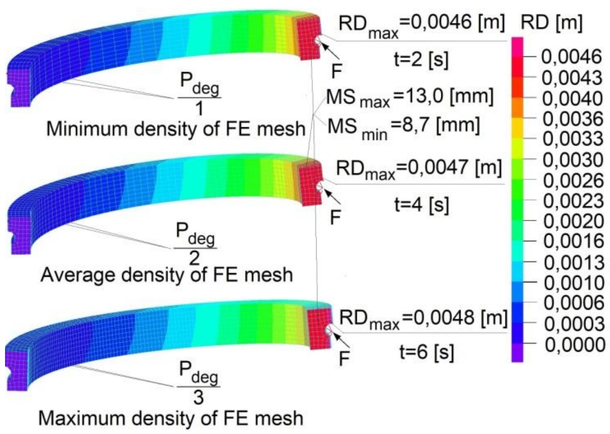

Fig. B2. Distributions of the displacements for the tested meshes of the slewing bearing ring model

The mesh size was defined by the maximum MS_{max} and minimum MS_{min} a distance between nodes of the finite element in a considered structure of an object. The calculation time, denoted by subol t in Figures B1 B2 B3, is given for all models tested. Calculations were performed using two processor cores of i5-4590, CPU 3,3 GHz and the memory of 1825 [MB]. Eight-nodal finite elements type 3D-Solid [27, 28] were used in the contact zone model. Due to the fact that in this model the contact problem is being resolved, the maximum effective stress for the permissible load of the contact zone (F_{dop}) in the direction indicated by the nominal contact angle (α_o) was adopted as a criterion for rating of convergence of the solutions. Distributions of the effective stress in the contact zone models are shown in Fig. B1. In all cases, the Bielajew zone is clearly visible, wherein the maximum effective stress σ_{omax} were identified. Based on the formulas presented in [34], the theoretical maximum effective stress σ_{omax}=185 [MPa] was calculated.

Satisfactory convergence was obtained for the maximum density of FE mesh. This model was used to determine a characteristic of the contact zone (Fig. 5).

The slewing bearing model contains several groups of finite elements with specific properties. Due to the method of definition mutual relations between these groups a control of the mesh sensitivity carried out for a geometry of the inner ring of the slewing bearing 1 (Fig. 3) and contact pair of a toothed rim 3 and a drive pinion 5. These objects are represented using three-dimensional finite elements. It should be noted that the beam element of the superelement (Fig. 4) has a common node with the bearing ring. This node in the bearing model is a connector between elements which replace of the balls and the bearing raceways. This discretization system means that a displacement of this node caused by the point action of a load will depend on density of a mesh determined in a cross-section of the ring. The method of compensating this numerical effect is shown in [2]. Thus, discretization errors of the cross-section of the rings are reduced by modifying the characteristics of the contact zone [2]. The adopted system of connecting superelements with rings enforces angular positioning of finite elements in accordance with a pitch of the balls. Therefore, the test of mesh sensitivity concerned the circumferential arrangement of the nodes. The presented bearing model takes into account the bending and torsion of rings therefore the maximum displacement RD_{max} of the ring loaded with a constant force F through one superelement was assumed as a control criterion for testing meshes.

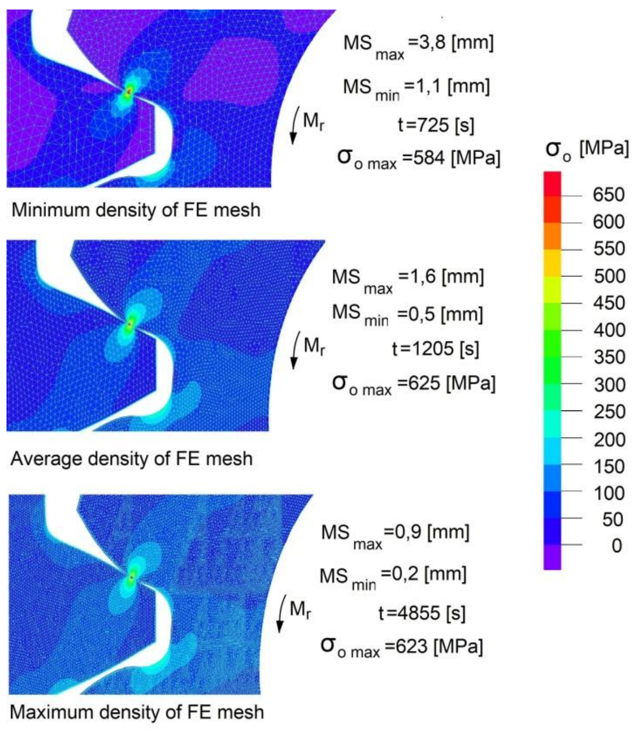

Fig. B3. Distributions of effective stress for the tested meshes of the contact zone model of a toothed rim and a drive pinion

The circumferential discretization pitch was set as a multiple of the angular pitch of the balls P_{deg}.The test calculation was performed for three different circumferential discretization pitch marked in Fig. B2. Based on the displacement distribution, it was found that a model with a minimum density of FE mesh is sufficient for bearing analysis.

Since the geometry of the gearing system is more complex than the geometry of the ring, the structure of a toothed rim and a drive pinion was modeled with twelve-nodal finite elements type

DOI 10.2478/ama-2025-0003

3D-Solid [27, 28].In this model, the focus was on determining the mesh sizes for the tooth pairs in contact when bearing is loaded [30]. Permissible effective stress in the contact zone for gears was set as criterion for rating of convergence of the solution. A value of this stress for the bearing material is σ_o=650 [MPa]. Based on this value, an allowable torque M_r=8717 [Nm] was calculated. This torqe was implemented in three contact zone models of a toothed rim and a drive pinion. The calculation results are presented in Fig. B3. Satisfactory convergence was obtained for the average density of FE mesh.

Based on the sensitivity analysis of the meshes, the model of slewing bearing cooperating with a drive pinion presented above was built. The statistical data of this model are summarized in Tab. B1.

Tab. B1. Statistical data of the FE model of the slewing bearing

The modeled object	Finite element type	Number of finite elements
The ball as a Superelement	Truss	128
	Beam	512
Inner ring	3D-Solid	3584
Outer ring	3D-Solid	3584
Bolts	Beam	84
Heads of the mounting bolts	3D-Solid	5040
Upper support structure	3D-Solid	3392
lower support structure	3D-Solid	3392
Płyta	3D-Solid	1
Toothed rim	3D-Solid	56340
Pinion	3D-Solid	37651

The calculation time necessary to determine one of the points of the static static carrying capacity curves was t=7120 [s].

REFERENCES

1. Aguirrebeitia J, Abasolo M, Aviles R, Bustos IF. General static load-carrying capacity for the design and selection of four contact point slewing bearings: finite element calculations and theoretical model validation. Finite Elem. Anal. Des. 2012; 55: 23-30. Available from: https://doi.org/10.1016/j.finel.2012.02.002
2. Śpiewak S. Methodology for calculating the complete static carrying capacity of twin slewing bearing. Mechanism and Machine Theory 2016; 101: 181–194. Available from: https://doi.org/10.1016/j.mechmachtheory.2016.03.017
3. Slewing Ring Turntable Bearings. Kaydon Corporation. Catalog 390, Muskegon. 2011.
4. Rothe Erde slewing berings. RotheErde GmbH. Dortmund. 2007.
5. INA Slewing rings. Catalogue 404, Schaeffler Technologies AG & Co. KG Herzogenaurach (Germany).
6. Potočnik R, Göncz P, Glodež S. Static capacity of a large double row slewing ball bearing with predefined irregular geometry. Mechanism and Machine Theory. 2013;64:67-79. Available from: https://doi.org/10.1016/j.mechmachtheory.2013.01.010
7. Śpiewak S. A peculiarity of determining a static carrying capacity for the one-row ball slewing bearing loaded the large radial force. Journal of KONES. 2016; 3: 533 - 540.
8. Li Y, Jiang D. Dynamic carrying capacity analysis of double-row four-point contact ball slewing bearing, Mathematical Problems in Engineering, 2015; PT.19: 1-7. Available from:10.1155/2015/850908
9. Smolnicki T, Derlukiewicz D, Stańco M. Evaluation of load distribution in the superstructure rotation joint of single-bucket caterpillar excavators. Automation in Construction. 2008;17:218–223.
10. He P, Hong R, Wang H, Lu C. Fatigue life analysis of slewing bearings in wind turbines. International Journal of Fatigue. 2018; 111: 233-242. Available from: https://doi.org/10.1016/j.ijfatigue.2018.02.024
11. Jaskot A, Śpiewak B, Śpiewak S. Influence of radial forces positively, negatively and perpendiculary directed on the static carrying capacity of the one row ball slewing bearing. Machine Dynamics Research. 2015; 3: 33 - 47.
12. Glodež S, Potočnik R, Flašker J, Computational model for calculation of static capacity and lifetime of large slewing bearing's raceway, Mechanism and Machine Theory. 2012;47:16-30. Available from: https://doi.org/10.1016/j.mechmachtheory.2011.08.010
13. Li Y, Wang R, Mao F. Calculation method for the static carrying curve of double-row different-diameter ball slewing bearings. Science Progress. 2023; 106(2). Available from: 10.1177/00368504231180026
14. Friederici V, Schumacher J, Clausen B, Influence of local differences in microstructure and hardness on the fatigue behaviour of a slewing bearing steel. Procedia Structural Integrity. 2021;31:8-14. Available from: https://doi.org/10.1016/j.prostr.2021.03.003
15. He P, Liu R, Hong R, Wang H, Yang G, Lu C. Hardened raceway calculation analysis of a three-row roller slewing bearing. International Journal of Mechanical Sciences. 2018; 137: 133-144. Available from: https://doi.org/10.1016/j.ijmecsci.2018.01.021.
16. Caesarendra W, Kosasih B, Tieu AK, Moodie CAS. Application of the largest Lyapunov exponent algorithm for feature extraction in low speed slewing bearing condition monitoring. Mechanical Systems and Signal Processing. 2015; January 50–51: 116-138. Available from: https://doi.org/10.1016/j.ymssp.2014.05.021
17. Caesarendra W, Kosasih B, Tieu AK, Zhu H, Moodie CAS, Zhu Q. Acoustic emission-based condition monitoring methods: Review and application for low speed slew bearing. Mechanical Systems and Signal Processing. 2016; 72–73: 134-159. Available from: https://doi.org/10.1016/j.ymssp.2015.10.020
18. Žvokelj M, Zupan S, Prebil I. EEMD-based multiscale ICA method for slewing bearing fault detection and diagnosis, Journal of Sound and Vibration. 2016; 26: 394-423. Available from: Available from: https://doi.org/10.1016/j.jsv.2016.01.046
19. Wang S, Chen J, Wang H, Zhang D. Degradation evaluation of slewing bearing using HMM and improved GRU. Measurement. 2019; 146: 385-395. Available from: https://doi.org/10.1016/j.measurement.2019.06.038
20. Heras I, Aguirrebeitia J, Abasolo M. Friction torque in four contact point slewing bearings: Effect of manufacturing errors and ring stiffness. Mechanism and Machine Theory. 2017; 112: 145-154. Available from: https://doi.org/10.1016/j.mechmachtheory.2017.02.009
21. Dindar A, Akkök M, Çalışkan M, Experimental Determination and Analytical Model of Friction Torque of a Double Row Roller Slewing Bearing, Journal of Tribology. 2017; 139(2): 021503, Available from: https://doi.org/10.1115/1.4033364
22. Babu S, Manisekar K. Experimental Study of Heat Distribution in Polished Bearing Surfaces for Design and Development of Large Diameter Slewing Ring Bearing for FBR. Procedia Engineering. 2014; 86: 350-358. Available from: https://doi.org/10.1016/j.proeng.2014.11.048
23. Amasorraina JI, Sagartzazu X, Damián J. Load distribution in a four contact-point slewing bearing. Mechanism and Machine Theory. 2003; 38: 479-496. Available from: https://doi.org/10.1016/S0094-114X(03)00003-X
24. Göncz P, Potočnik R, Glodež S. Load capacity of a three-row roller slewing bearing raceway. Procedia Engineering. 2011; 10: 1196-1201. Available from: https://doi.org/10.1016/j.proeng.2011.04.199
25. Aguirrebeitia J, Plaza J, Abasolo M, Vallejo J. Effect of the preload in the general static load-carrying capacity of four-contact-point slewing

bearings for wind turbine generators: theoretical model and finite element calculations. Wind Energ. 2014; 17: 1605–1621. Available from: https://doi.org/10.1002/we.1656
26. Kania L, Śpiewak S. English title: Determining the reactions of balls slewing bearing mounted in working struktures of the single-bucket excavator. Polish title: Wyznaczanie reakcji kulek łożyska wieńcowego osadzonego w strukturach roboczych koparki jednonaczyniowej. Zeszyty Naukowe Transport. Politechnika Śląska. 2014; 83: 127-136.
27. ADINA.Theory and Modeling Guide. Vol. 1: ADINA Solids & Structures. ADINA R&D Inc. Watertown. 2012.
28. Bathe KJ, Finite Element Procedures. Prentice-Hall. Inc. Simon & Schuster/A Viacom Company Upper Saddle River. New Jersey. 1996.
29. Hwang SC, Lee JH, Lee DH, Han SH, Lee KH. Contact stress analysis for a pair of mating gears. Mathematical and Computer Modelling. 2013; 57:40-49. Available from: https://doi.org/10.1016/j.mcm.2011.06.055
30. Li S. Effect of addendum on contact strength, bending strengthand basic performance parameters of a pair of spur gears. Mechanism and Machine Theory. 2008; 43: 1557–1584.
31. DIN/ISO – 898.
32. Smolnicki T, Rusiński E. Superelement-based modeling of load distribution in large-size slewing bearings. Journal of Mechanical Design. 2007; 129: 459-463.
33. Kania L., Śpiewak S. Współczynnik krotności łożysk wieńcowych podwójnych. Acta Mechanica et Automatica. 2009;3(1): 65-67.
34. Brändlein J, Eschmann P, Hasbargen L, Weigand K, Die Wälzlagerpraxis. Vereinigte Fachverlag GmbH. 1998. Mainz.
35. Smolnicki T,. Modelling, computing, and analyzing large-size rotary joints; In: Sokolski, M. (eds) Mining Machines and Earth-Moving Equipment. Springer. 2020. Cham. Available from: https://doi.org/10.1007/978-3-030-25478-0_3
36. Sokolski P, Smolnicki T. A method for monitoring the technical condition of large-scale bearing nodes in the bodies of machines operating for extended periods of time. Energies. 2021;14:6637. Available from: https://doi.org/10.3390/en14206637
37. He P, Qian Q, Wang Y, Liu H. Guo E, Wang H. Influence of finite element mesh size on the carrying capacity analysis of single-row ball slewing bearing. Advances in Mechanical Engineering. 2021; 13: 1–12.
38. Kania L, Krynke M, Mazanek E. A catalogue capacity of slewing bearings. Mechanism and Machine Theory. 2012; 58: 29–45. Available from: https://doi.org/10.1016/j.mechmachtheory.2012.07.012

Szczepan Śpiewak: https://orcid.org/0000-0002-7057-8356